

Role of codopant oxygen in erbium-doped silicon

Jun Wan, Ye Ling, Qiang Sun, and Xun Wang*

Surface Physics Laboratory (National Key Laboratory), Fudan University, Shanghai 200433, China

(Received 27 October 1997)

The structural and electronic properties of Er-doped Si system with and without the codopant of oxygen are studied theoretically by using the first principle discrete variational cluster method based on the *ab initio* local-density approximation. Several cluster models are adopted for simulating an Er point defect located at different sites in the Si host with high symmetry. The role of oxygen is especially investigated. The results show that the presence of oxygen changes the binding energy drastically, i.e., a positive energy is needed for the incorporation of an Er defect into Si, but with the existence of surrounding oxygen atoms a negative binding energy is found. This could explain the experimental results that the presence of oxygen can enhance the effective solubility of Er in Si. The electronic structures for different Si:Er configurations with and without oxygen are calculated. Differences are found for the two cases in their density of states and charge distributions.

[S0163-1829(98)00940-0]

I. INTRODUCTION

Er-doped Si has been considered as a promising Si-based light-emitting material since the first report of photoluminescence from Si:Er in 1983.¹ The rare-earth Er ion is well known to emit photons at the wavelength around 1.53 μm , which corresponds to the absorption minima of the optical fibers. Extensive experimental studies have been performed on the Si:Er system. It has been found² that codoping the sample with oxygen plays an important role on the luminescence of Er in Si. First, the presence of O can enhance the effective solid solubility of Er in Si.³⁻⁵ Also, the site location and coordination of Er in Si are altered by the presence of O.⁶⁻⁸ Another role is that the presence of O can influence the deep-level properties of Er in crystalline Si.^{9,10} Recently, room-temperature photoluminescence as well as electroluminescence have been achieved for Er and O codoped Si.^{11,12}

Up to now to our knowledge, few theoretical studies have been done on the Si:Er system. Most of the theoretical calculations treated the Er element within the framework of “frozen 4f” orbital conception, in which the 4f electrons of Er are considered as core electrons screened by the 5s, 5p filled shells and 6s, 5d valence orbitals. Thus, the interaction between Er 4f electrons and the valence electrons of host materials is ignored. DeLerue and Lannoo¹³ studied the substitutional Er in Si by using a tight-binding Green’s-function technique. The rare-earth 4f states were treated as frozen core acting as resonant states in the Si valence band. Another theoretical simulation was done by Needels, Schluter, and Lannoo.¹⁴ To our knowledge, this is the only work that calculated the total energy of different configurations consisting of Er and Si atoms. The 4f electrons were also treated as core electrons. It was found that Er³⁺ at a tetrahedral interstitial site is the favorable configuration with the lowest energy. Yassievich and Kimerling¹⁵ proposed that Er in Si behaves like an isolated ion Er³⁺, with its 4f level located 20 eV below the Er 5d level, and thus deepened in the Si valence band.

However, the “frozen 4f” approximation in considering

the interaction of Er and its host materials is not always unquestionable. The earlier calculation of rare-earth element chemisorption on the Si surface illustrated that the 4f energy levels would be raised due to the bonding with Si atoms.¹⁶ The hybridization of 4f orbitals of rare-earth elements with an Si valence band has also been verified experimentally by the photoemission measurements.¹⁷ Recently *ab initio* self-consistent field electronic-state calculations carried out for isolated interstitial Er impurities in Si also showed that the Er 4f orbitals have to be treated as valence states in order to describe the interactions between impurity and host atoms because Si is a covalent bonded semiconductor.¹⁸

Moreover, the role of O on the atomic configuration and electronic structure of Er in Si has not been treated theoretically, as far as we know.

In this paper, the electronic structures of Er in Si, as well as the influences of oxygen on the total energy and electronic structure, are investigated. Er 4f orbitals are treated as valence electrons together with Er 5d and 6s orbitals in the calculation.

II. METHODS AND MODELS

The method used in the present work is what is known as the discrete-variational-self-consistent multicenter-multipolar (DV-SCM) method. In this DV method, a SCM representation of the density is introduced. The Hamiltonian matrix elements and the overlap matrix elements (and, therefore, the wave functions and charge densities) were all given by numerical values on a set of sampling points. The wave functions of the cluster were expanded variationally in symmetrized atomic basis functions, which were generated self-consistently in numerical form. The detailed description of this method could be found in Ref. 19. The potentials adopted were Hedin and Lundqvist exchange-correlation terms.²⁰ In our calculations, the 4f, 5d, and 6s electrons of the Er atom, the 2s, 2p electrons of the O atom, the 3s, 3p electrons of the Si atom, and the 1s electron of the H atom were treated as valence electrons.

The exact geometry of defects in a host is difficult to

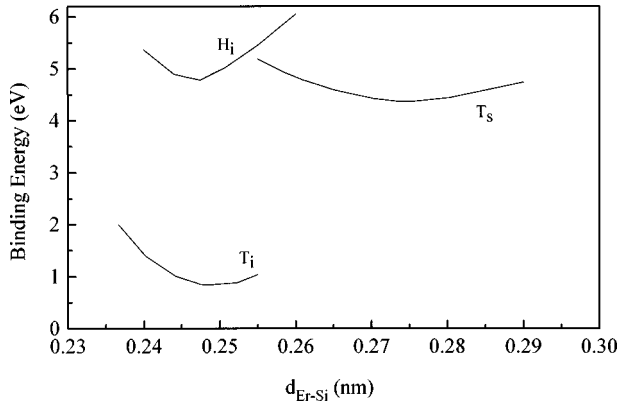


FIG. 1. The binding energy vs Er-Si distance for three different configurations H_i , T_i , and T_s .

determine. Cluster models provide a flexible approach for dealing with this problem. For the substitutional Er impurity the cluster used comprises a central Er atom surrounded by 34 Si atoms and 36 H terminators. This configuration is denoted as T_s . The tetrahedral and hexagonal interstitial Er impurities are simulated by two clusters, which comprise 30 Si atoms, 40 H atoms, and 38 Si atoms, 44 H atoms, respectively. One Er atom is placed at the center of these clusters. These configurations are denoted as T_i and H_i , respectively. If the oxygen atoms are added into the above three structures, 4, 4, and 6 oxygen atoms are placed at the interstitial sites in Si as the nearest neighbors of the Er atom according to point-group symmetries, and these configurations with O are denoted as $T_s + O$, $T_i + O$, and $H_i + O$, respectively. The point-group symmetries of these three configurations are T_d , T_d , and C_{3v} , respectively. These clusters are chosen in order to take into consideration the relaxation of one shell of Si atoms and O atoms. The configuration optimization processes are carried out with the symmetry of the clusters kept unchanged in the minimization.

III. RESULTS AND DISCUSSION

A. Total energies

The binding energy of an Er atom in Si is defined as

$$E = E(\text{Er} + n\text{Si} + n'\text{H})_{\text{clu}} - [E(\text{Er}) + E(n\text{Si} + n'\text{H})_{\text{clu}}], \quad (1)$$

and with the presence of O, the binding energy is

$$E' = E(\text{Er} + n\text{Si} + n'\text{H} + n''\text{O})_{\text{clu}} - [E(\text{Er}) + n''E(\text{O}) + E(n\text{Si} + n'\text{H})_{\text{clu}}], \quad (2)$$

where clu refers to the cluster and n , n' , and n'' are the numbers of Si, H, and O atoms, respectively. For substitutional configuration, $E(n\text{Si} + n'\text{H})_{\text{clu}}$ in Eq. (1) is defined as follows:

$$E(n\text{Si} + n'\text{H})_{\text{clu}} = E[(n+1)\text{Si} + n'\text{H}]_{\text{clu}} - E(\text{Si}). \quad (3)$$

The calculated binding energies of an Er atom in Si as a function of Er-Si distance ($d_{\text{Er-Si}}$) for the three configurations without O are plotted in Fig. 1. The optimized distances between Er and Si atoms are 0.248, 0.275, and 0.247 nm for T_i , T_s , and H_i configurations, respectively. Among them,

TABLE I. The binding energies for different configurations.

Configuration	Binding energy (eV)	$d_{\text{Er-Si}}$ (nm)	$d_{\text{Er-O}}$ (nm)
T_i	0.84	0.248	
T_s	4.38	0.275	
H_i	4.78	0.247	
$T_i + O$	-12.96	0.251	0.247
$T_s + O$	-14.15	0.386	0.218
$H_i + O$	-15.28	0.260	0.218

$d_{\text{Er-Si}}$ of the T_s configuration is closer to the sum of Er and O covalent bond lengths (0.274 nm). The binding energies for T_i , T_s , and H_i configurations are 0.84, 4.38, and 4.78 eV, respectively. They are all positive values indicating that the incorporation of Er in Si requires additional energies. This might be one of the reasons that cause the rather low solubility of Er in Si observed by the experimental measurement ($\sim 2 \times 10^{16}/\text{cm}^3$ at 900 °C).²¹

The most favorable configuration is T_i , whose binding energy is 0.84 eV with $d_{\text{Er-Si}} = 0.248$ nm. The results calculated by Needels, Schluter, and Lannoo¹⁴ showed that Er with a trivalent oxidation state at T_i configuration is the lowest-energy configuration. The distance between Er and the nearest Si is 0.248 nm, which agrees well with our result.

When O is incorporated, there are drastic changes in binding energies, as shown in Table I. The binding energies for $T_i + O$, $T_s + O$, and $H_i + O$ configurations are -12.96, -14.15, and -15.28 eV, respectively. They are all negative values. It means that the codoping of Er and O is an exothermal process, which is thus in favor of enhancing the effective solubility of Er in Si as being achieved in experiments.³⁻⁵ Also, the incorporated efficiency of O could be enhanced with the presence of Er, too. In fact, it has been directly observed that the incorporated oxygen concentration depends strongly on the incorporated Er concentration; the higher the Er concentration, the higher the level of oxygen incorporation in the Si film.²²

With the presence of oxygen, $H_i + O$ is found to be the most stable configuration. The calculated distance between Er and Si is 0.260 nm, and that of Er and O is 0.218 nm. This is consistent with the experimental results.⁶ The extended x-ray absorption fine structure showed that in Er-implanted oxygen-containing Si samples the structure is a local sixfold coordination of O atoms around Er at an average distance of 0.225 nm. The electron paramagnetic resonance and Rutherford backscattering measurements⁸ have shown that Er incorporation in Si with a concomitant O codoping produces a structure consisting of an Er residing in an interstitial site with six O atoms surrounding it.

It is well known that the binding energy of oxygen in Si is negative. To judge whether the above energy lowering is all due to the interaction between O and Si, the binding energy of six interstitial O atoms in H_i configuration is calculated. The result shows that its binding energy is -11.99 eV. Its absolute value is smaller than that for $H_i + O$ configuration shown in Table I (-15.28 eV). So, the Er-O interaction may be also in response to the binding energy lowering.

In order to investigate the nature of bonding, the charge-contour plots containing Si, O (if codopant with) and the central Er atom of H_i and $H_i + O$ configurations are given as

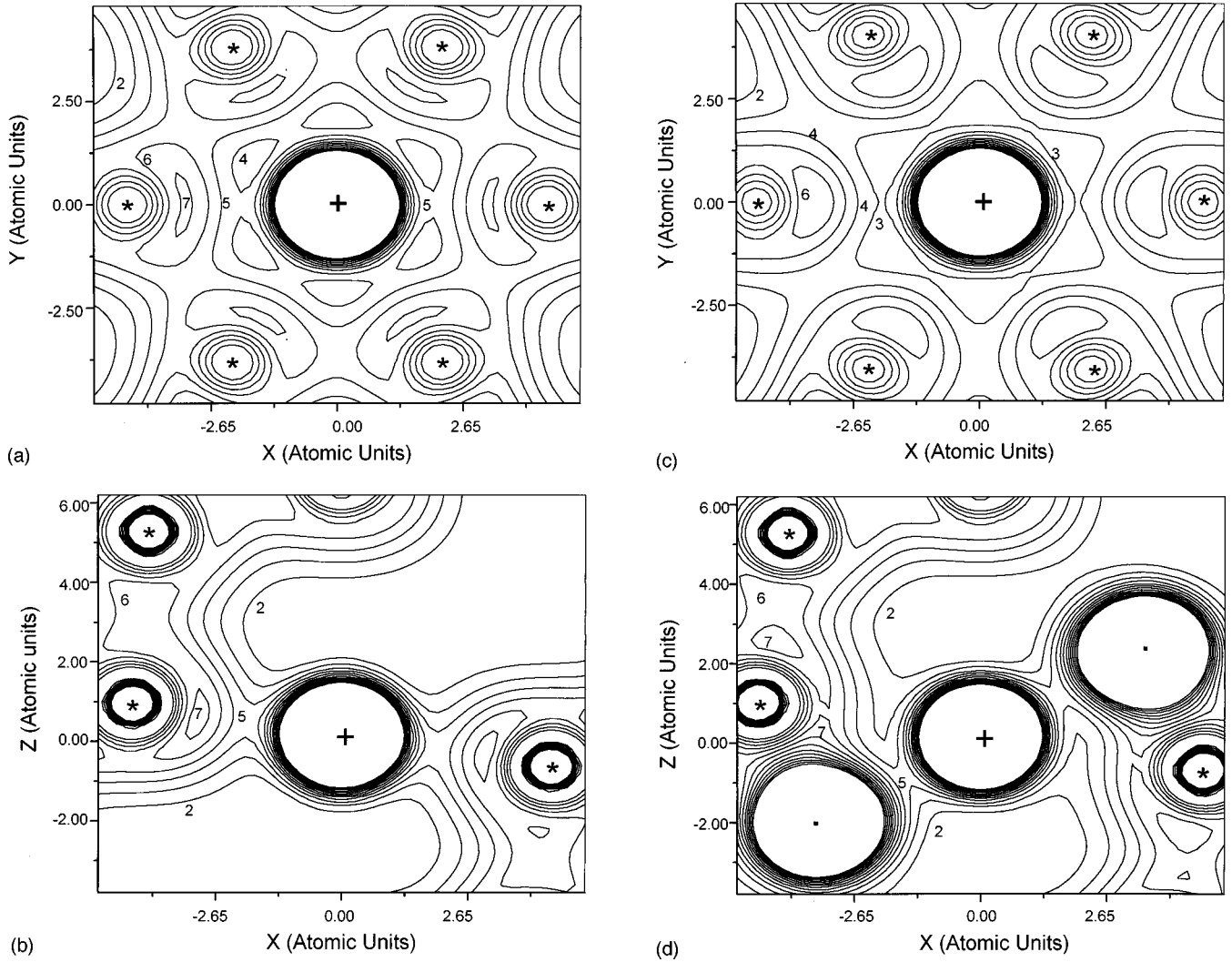


FIG. 2. The contour plots of charge densities, (a) in a horizontal xy plane containing a six Si atom ring and an Er atom for an H_i configuration; (b) in a vertical xz plane that is perpendicular to (a) for an H_i configuration; (c) in a horizontal xy plane containing a six Si atom ring and an Er atom for an $H_i + O$ configuration; (d) in a vertical xz plane that is perpendicular to (c) containing two oxygen atoms for an $H_i + O$ configuration. Contour intervals are 1.

shown in Fig. 2. In these two configurations, the nearest neighbor of the central Er atom is a zigzag hexagonal ring of Si atoms. Two planes are chosen to illustrate the charge-contour plots. An xy plane passes through the central Er atom with three nearest-neighbor atoms above it and the other three nearest-neighbor atoms below it, as shown in Figs. 2(a) and 2(c). Another plane is a vertical yz plane. It passes through the central Er atom, two Si atoms in the zigzag Si ring, and a Si atom located at higher place, as shown in Fig. 2(b). It will pass through two oxygen atoms with the presence of O [see Fig. 2(d)]. The position of the Er atom is denoted by a plus sign. The positions of the neighboring Si and O atoms are denoted by stars and dots, respectively. For pure Si the charge density in the middle of Si-Si bond (which is not plotted here), is about seven (in the unit of $10^{-2} e/a_0^3$, where a_0 is the Bohr radius). When an Er atom is put at the center of a Si ring, the charge distribution between Si-Si is slightly distorted and weakened. The numerical value along Si-Si changes to ~ 6 . Dense mappings (~ 5) between Er and Si atoms can be seen clearly in Figs. 2(a) and 2(b). With the presence of oxygen, it can be seen from Fig. 2(c) that the

charge distribution between Er and Si becomes weaker as compared with Fig. 2(a). The charge distribution between Si-Si is less distorted; however, its numerical value changes from six in Fig. 2(a) to four in Fig. 2(c). This is due to the interaction between Si and O as seen from Fig. 2(d), where a denser mapping is found between Si and O. The numerical value is about seven. In Fig. 2(d) there also exhibits a dense mapping (~ 5) between Er and O atoms, which is stronger than that of Er-Si [~ 3 , see Fig. 2(c)], which may infer that the interactions between Er and O atoms are stronger than that of Er-Si. So the codopant O atoms have interactions not only with Si but also with Er. Both contribute to the binding energy lowering.

B. Electronic structures

The calculated electronic configurations of Er for different structural configurations are shown in Table II. Due to the covalent effect, the number of electrons in Er $4f$, $5d$, and $6s$ orbitals are significantly different from that in the pure ion model. The numbers of $4f$ electrons are no longer

TABLE II. The electronic configurations and charge transfers of Er for different structures.

Structure	Atomic configuration of Er	Charge transferred from Er (e)	Charge gain by each O atom (e)
T_i	$4f^{11.41}5d^{1.90}6s^{0.36}$	0.32	
T_s	$4f^{11.44}5d^{1.30}6s^{0.37}$	0.89	
H_i	$4f^{11.42}5d^{1.84}6s^{0.28}$	0.46	
$T_i + O$	$4f^{11.40}5d^{1.77}6s^{0.53}$	0.30	0.36
$T_s + O$	$4f^{11.33}5d^{1.29}6s^{0.12}$	1.26	0.46
$H_i + O$	$4f^{11.46}5d^{1.91}6s^{0.05}$	0.58	0.40

integers of 11 or 12. A large portion of $6s$ electrons transfers to the $5d$ orbital, which was originally empty. This means that the valence electrons mainly show a $5d$ -like character. Besides the $4f$ and $6s$ orbitals, the $5d$ states of Er play an important role in describing the interaction between the Er impurity and Si crystal.

When relatively stable configurations are formed, electrons transfer from Er to Si and O atoms. This trend is consistent with the Pauli electronegativities of Er, Si, and O which are 1.3, 1.8, and 3.5, respectively. The charge transfers are listed in Table II. Without the presence of O, Er lost 0.32, 0.89, and 0.46 electrons in T_i , T_s , and H_i configurations, respectively. With the presence of O, the charges transferred from Er are 0.30, 1.26, and 0.58 e^- in $T_i + O$, $T_s + O$, and $H_i + O$, respectively. The charges transferred from Er for $T_s + O$ and $H_i + O$ configurations become larger. While for T_i configuration, the charge transferred from Er decreases slightly. This decline may be connected with the fact that the distance between Er and O is 0.247 nm, which is greater than the sum of the Er and O covalent radius of 0.223 nm. The O atoms gain charges not only from Er, but also from Si atoms. For example, six O atoms get 2.4 electrons in $H_i + O$ configurations, while the charge transferred from Er to O and Si atoms is only 0.58 e^- .

Figures 3, 4, and 5 are the calculated densities of states (DOS) for T_i , H_i , and $H_i + O$ configurations. Since the cluster model results in discrete energy levels rather than a continuous distribution curve, Gaussian broadening was added to describe the DOS. A broadening parameter of 0.2 eV was adopted. In these figures, the top of the Si valence band is chosen as the origin of energy. The vertical line represents the highest occupied energy level. It should be noted that due to the limit size of the cluster the calculated energy gap of Si is about 1.6 eV, which is larger than the experimental data. The energy positions in DOS are thus only qualitatively meaningful. In order to identify the contributions of different orbitals to the DOS, the partial densities of states (PDOS) of Er $4f$, $5d$, $6s$, and O $2s$, $2p$ are also given. In these figures, the PDOS are also broadened.

Without the presence of O, the lowest energy configuration is T_i . In Fig. 3(a) there exist two peaks, a and b . From the PDOS, peaks a and b are basically contributed by the Er $4f$ and $5d$ orbitals, respectively. Peak a is a localized state in the Si band gap. Peak b is a shallow resonant state lying in the conduction band of Si. There is no Er $5d$ -derived states in the gap. Needels, Schluter, and Lannoo¹⁴ also showed that the bonding combination of the Er $5d$ orbitals and the Si

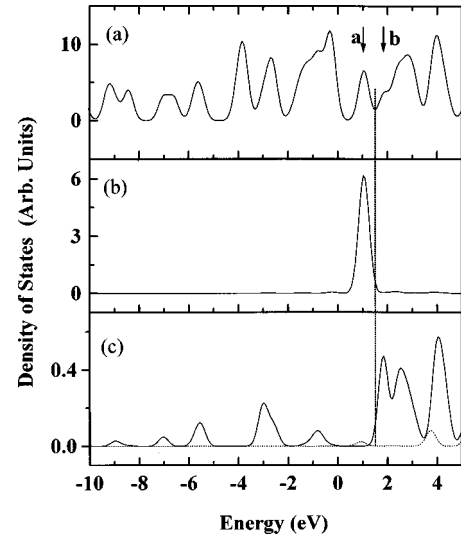


FIG. 3. (a) Total density of states (TDOS) for configuration T_i , (b) PDOS of Er $4f$, and (c) PDOS of Er $5d$ (solid curve) and Er $6s$ (dashed curve).

antibonding orbitals lies high in the gap. However, as this level is primarily derived from the Si conduction-band edge, they could not judge whether this state is a shallow resonant state in the conduction band or a gap state. Our results show that this state is more likely a shallow resonant state. According to Yassievich and Kimerling¹⁵ the probability of an Auger excitation of Er in Si would be very low if there is no additional localized electron state in the forbidden gap except Er $4f$. Our results show that this is the case for pure Er in Si.

When O is incorporated into Si, the most stable configuration is $H_i + O$. In order to investigate the influence of oxygen on electronic structures, the DOS of H_i and $H_i + O$ configurations are plotted in Figs. 4 and 5, respectively. It can be seen from these two figures that the influences of oxygen on the PDOS of Er $4f$ and $5d$ are not significant. Er $4f$ -like levels are still located in the gap similar to the former two configurations. A major change of the electronic structure is

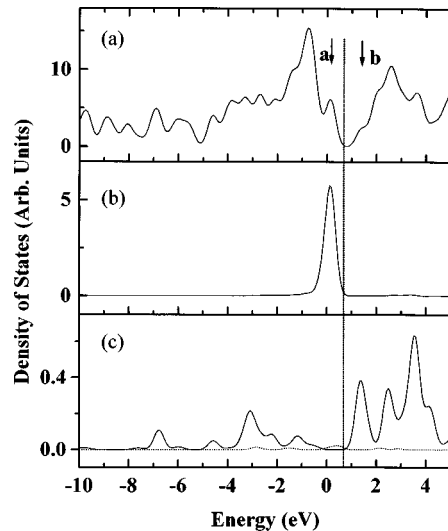


FIG. 4. (a) TDOS for configuration H_i , (b) PDOS of Er $4f$, and (c) PDOS of Er $5d$ (solid curve) and Er $6s$ (dashed curve).

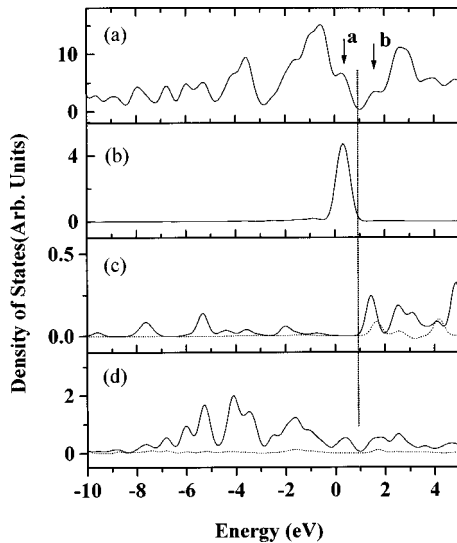


FIG. 5. (a) TDOS for configuration $H_i + O$, (b) PDOS of Er $4f$, (c) PDOS of Er $5d$ (solid curve) and Er $6s$ (dashed curve), (d) PDOS of O $2p$ (solid curve) and O $2s$ (dashed curve).

the upward shift of Er $6s$ levels into the conduction band. O $2s$ orbitals lie deep in the valence band and are not totally plotted here. O $2p$ orbitals have interaction with Er $5d$ orbitals below the conduction band. Thus, the density of peak b is enhanced as compared with Fig. 4. This gap-state bonding combination of the Er $5d$ orbitals, O $2p$ orbitals, and Si $2p$ electrons lies high in the gap, about 0.3 eV below the conduction-band edge. The deep-level transient spectroscopy measurement¹⁰ showed that in O and Er coimplanted Si a defect level with an activation energy of $E_c - E_t \sim 0.15$ eV was observed (E_c and E_t are the conduction-band edge and the deep trap level, respectively). This energy level may correspond to the $E_c - 0.3$ eV energy level calculated here.

From the above electronic structures, it can be seen that Er $5d$ have distributions deep in the valence band, while the

Er $6s$ levels lie high in the conduction band. This is consistent with the electronic configurations of Er listed in Table II. Er $4f$ -like levels lie near the edge of the valence band. The reason is that the compression of the charges stored in the delocalized Er $6s$ and Er $5d$, due to the solid-state environment, increases the Coulomb interaction between $4f$ and external electrons, and as a result the $4f$ -like states rise in energy to the point of overlapping the valence-band states while remaining localized.¹⁷

IV. CONCLUSIONS

The role of codopant oxygen on the atomic structure and electronic states in Er-doped Si is investigated theoretically. The results show that it is reasonable to treat the Er $4f$ electrons as valence electrons, and the hybridization among Er $4f$, $5d$, and $6s$ orbitals is responsible for the interaction between the Er and Si host.

From the total-energy and electronic structure calculations for several clusters proposed according to the point-group symmetry, O atoms have at least two roles in the Si:Er system. First, the presence of O can greatly lower the binding energy, thus in favor of the incorporation into Si. The energy lowering comes from not only the interactions between O and Si atoms, but also the interactions between O and Er atoms. As a consequence, $H_i + O$ configurations, i.e., one Er atom located at the hexagonal interstitial configuration and surrounded by six O atoms, is the most stable one. Another role of O is to change the electronic states. The Er $6s$ levels move up into the conduction band and are almost unoccupied. The Er $5d$ orbitals are hybridized with O $2p$ and Si $2p$ electrons forming a gap state near the Si conduction-band edge.

ACKNOWLEDGMENTS

This work was supported by the State Commission of Science and Technology and the National Natural Science Foundation of China.

*Author to whom correspondence should be addressed.

¹H. Ennen, J. Schneider, G. Pomrenke, and A. Axmann, Appl. Phys. Lett. **43**, 943 (1983).

²J. Michel, J. L. Benton, R. F. Ferrante, D. C. Jacobson, D. J. Eaglesham, E. A. Fitzgerald, Y.-H. Xie, J. M. Poate, and L. C. Kimerling, J. Appl. Phys. **70**, 2672 (1991).

³P. S. Andry, W. J. Varhue, F. Ladipo, K. Ahmed, E. Adams, M. Lavoie, P. B. Klein, R. Hengehold, and J. Hunter, J. Appl. Phys. **80**, 551 (1996).

⁴R. Serna, M. Lohmeier, P. M. Zagwijn, E. Vlieg, and A. Polman, Appl. Phys. Lett. **66**, 1385 (1995).

⁵J. S. Custer, A. Polmn, and H. M. van Pinxteren, J. Appl. Phys. **75**, 2809 (1994).

⁶D. L. Adler, D. C. Jacobson, D. J. Eaglesham, M. A. Marcus, J. L. Benton, J. V. Poate, and P. H. Citrin, Appl. Phys. Lett. **61**, 2181 (1992).

⁷A. Kozanecki, R. J. Wilson, B. J. Sealy, J. Kaczanowski, and L. Nowicki, Appl. Phys. Lett. **67**, 1847 (1995).

⁸J. D. Carey, J. F. Donegan, R. C. Barklie, F. Priolo, G. Franzo, and S. Coffa, Appl. Phys. Lett. **69**, 3854 (1996).

⁹S. Libertino, S. Coffa, G. Franzo, and F. Priolo, J. Appl. Phys. **78**, 3867 (1995).

¹⁰F. Priolo, G. Franzo, S. Coffa, A. Polman, S. Libertino, R. Barklie, and D. Carey, J. Appl. Phys. **78**, 3874 (1995).

¹¹J. Palm, F. Gan, B. Zheng, J. Michel, and L. C. Kimerling, Phys. Rev. B **54**, 17 603 (1996).

¹²G. Franzo, S. Coffa, F. Priolo, and C. Spinella, J. Appl. Phys. **81**, 2784 (1997).

¹³C. DeLerue and M. Lannoo, Phys. Rev. Lett. **67**, 3006 (1991).

¹⁴M. Needels, M. Schluter, and M. Lannoo, Phys. Rev. B **47**, 15 533 (1993).

¹⁵I. N. Yassievich and L. C. Kimerling, Semicond. Sci. Technol. **8**, 718 (1993).

¹⁶Ye Ling and Xie Xide, Acta Phys. Sin. **37**, 1593 (1988).

¹⁷G. Rossi, Surf. Sci. Rep. **7**, 1 (1987).

¹⁸F. Gan, L. V. C. Assali, and L. C. Kimerling, Mater. Sci. Forum **196-201**, 579 (1995).

¹⁹Ye Ling, A. J. Freeman, and B. Delly, Phys. Rev. B **39**, 10 144 (1989); B. Delly and D. Ellis, J. Chem. Phys. **76**, 1949 (1982).

²⁰L. Hedin and B. I. Lundqvist, J. Phys. C **4**, 2064 (1971).

²¹F. Y. G. Ren, J. Michel, Q. Sun-Paduano, B. Zheng, H. Kitagawa, D. C. Jacobson, J. M. Poate, and L. C. Kimerling, in *Rare Earth Doped Semiconductors*, edited by G. S. Pomrenke, P. B. Klein,

and D. W. Langer, MRS Symposia Proceedings No. 301 (Materials Research Society, Pittsburgh, 1993), p. 87.

²²Morito Matsuoka and Shun-ichi Tohno, J. Appl. Phys. **78**, 2751 (1995).